Check for updates

Received: 29 November 2021 | Accepted: 3 January 2022

DOI: 10.1111/pce.14285

ORIGINAL ARTICLE

Plant, Cell & Environment | WILEY

Rice increases phosphorus uptake in strongly sorbing soils by intra-root facilitation

Christian W. Kuppe[1,2] | Guy J. D. Kirk[3] | Matthias Wissuwa[4] | Johannes A. Postma[1]

[1]Forschungszentrum Jülich GmbH, Institute of Bio- and Geosciences – Plant Sciences (IBG-2), Jülich, Germany

[2]RWTH Aachen University, Aachen, Germany

[3]School of Water, Energy and Environment, Cranfield University, Cranfield, MK43 0AL, UK

[4]Crop, Livestock and Environment Division, Japan International Research Center for Agricultural Sciences (JIRCAS), Tsukuba, Japan

Correspondence

Christian W. Kuppe, Forschungszentrum Jülich GmbH, Institute of Bio- and Geosciences – Plant Sciences (IBG-2), Jülich 52425, Germany.
Email: c.kuppe@fz-juelich.de

Funding information

Biotechnology and Biological Sciences Research Council; OCP (Cranfield-Rothamsted-UM6P Collaboration Grant); Helmholtz-Gemeinschaft; Deutsche Forschungsgemeinschaft (DFG, German Research Foundation), Grant/Award Number: 491111487

Abstract

Upland rice (*Oryza sativa*) is adapted to strongly phosphorus (P) sorbing soils. The mechanisms underlying P acquisition, however, are not well understood, and models typically underestimate uptake. This complicates root ideotype development and trait-based selection for further improvement. We present a novel model, which correctly simulates the P uptake by a P-efficient rice genotype measured over 48 days of growth. The model represents root morphology at the local rhizosphere scale, including root hairs and fine S-type laterals. It simulates fast- and slowly reacting soil P and the P-solubilizing effect of root-induced pH changes in the soil. Simulations predict that the zone of pH changes and P solubilization around a root spreads further into the soil than the zone of P depletion. A root needs to place laterals outside its depletion- but inside its solubilization zone to maximize P uptake. S-type laterals, which are short but hairy, appear to be the key root structures to achieve that. Thus, thicker roots facilitate the P uptake by fine lateral roots. Uptake can be enhanced through longer root hairs and greater root length density but was less sensitive to total root length and root class proportions.

KEYWORDS

coupled transport model, phosphate, phosphorus uptake efficiency, rhizosphere pH, slow sorption, solubilization, upscaling

1 | INTRODUCTION

Deficiency of phosphorus (P) is one of the main constraints to crop production on highly weathered soils of the humid tropics (Alewell et al., 2020). Owing to the high content of iron and aluminium oxides in the clay fractions of such soils, added P becomes strongly sorbed on soil surfaces and is therefore largely unavailable to plant roots. However, certain plant species—exemplified by upland rice (*Oryza sativa*)—are efficient in extracting this strongly sorbed P. There are large differences in tolerance of low P availability in the upland rice germplasm (Rose et al., 2013; Vandamme et al., 2016) and there has been progress in mapping the associated genes (Gamuyao et al., 2012; Mori et al., 2016; Schatz et al., 2014). However, the mechanisms involved are poorly understood (Nestler & Wissuwa, 2016; Wissuwa et al., 2020). Genotypes differ in total P-uptake, P uptake per unit root surface area, and biomass per amount of P taken up—that is, the internal P use efficiency (Wissuwa et al., 2015, 2020). Mathematical models are needed to describe the underlying mechanisms. In this paper, we develop such a model, focusing on the processes involved in P uptake.

This is an open access article under the terms of the Creative Commons Attribution License, which permits use, distribution and reproduction in any medium, provided the original work is properly cited.
© 2022 The Authors. *Plant, Cell & Environment* published by John Wiley & Sons Ltd.

Four factors potentially influence plant P uptake and need to be considered: (1) root length, diameter, architecture, and coverage with hairs, as these affect the surface area available for P uptake; (2) the P uptake per unit surface area of roots and hairs; (3) root-induced changes in the soil that affect the solubility of P; and (4) the effects of rhizosphere microbes and mycorrhizal fungi. Current understanding of these factors for upland rice is as follows.

First, root architecture and morphology. The upland rice root system comprises large numbers of roots which are classified into crown, seminal, L- and S-type lateral roots. S-types are short and fine lateral roots (<1 cm length; <80 μm diameter) unique to rice (Yamauchi et al., 1987) and typically double the total length of a root system (Wissuwa et al., 2020). The crown and lateral roots, including the fine S-types, produce hairs. Recent 3D modelling, allowing for soil transport, uptake limitations, S-type lateral roots, and hairs, shows that the P cost of those fine laterals is recovered within a day of their formation (Gonzalez et al., 2021). They are therefore efficient in the use of P.

Second, the P uptake per unit root surface area. Conventional models of P uptake treat individual roots as 'sinks' to which P is delivered by transport through the soil solution (Kuppe et al., 2022). The sink strength is modelled as a function of P concentration in solution at the root surface and the activity of P uptake transporters in the root membrane. Such models greatly under-predict P uptake by upland rice grown in strongly P-sorbing soils, both when root architecture is (De Bauw et al., 2020; Gonzalez et al., 2021) and is not considered (Kirk et al., 1999). In strongly sorbing soils, P concentrations in the soil solution can be so low that even high-affinity transporters may still be slow in taking it up. Rates of transport through the soil by diffusion are, however, even slower (note rates of mass flow in the transpiration stream are negligible at these P concentrations). The conventional models underestimate P uptake even when it is assumed that the root reduces the P concentration at its surface to zero. This suggests that other processes, not allowed for in the conventional models, are important.

Third, root-induced solubilization. Solubilization of P through the secretion of low molecular weight organic acid anions, such as citrate and malate, is widely discussed (Hinsinger et al., 2011; Hoffland, 1992; Oburger et al., 2009). For rice, Kirk et al. (1999) used a model developed by Kirk (1999) and calculated the rates of citrate secretion from roots required to explain the measured rates of P uptake. The P-solubilizing effect of citrate and the rate of citrate decomposition were determined experimentally. However, the measured effluxes of citrate and other P-solubilizing organic exudates from rice roots (Wissuwa, 2005) are much smaller than required. Likewise, there is no evidence for organic P solubilization by release of phosphate enzymes from upland rice roots (Hedley et al., 1994) or genotypic differences in phosphatase secretion (Rakotoson et al., 2020). We, therefore, exclude the role of organic acids or phosphatases in P uptake.

A further potential solubilization mechanism is by root-induced pH changes in the soil. Roots that take up nitrogen as nitrate (NO_3^-) tend to take up an excess of anions over cations, balanced by the release of bicarbonate (HCO_3^-) anions, so causing an increase in rhizosphere pH (Dijkshoorn et al., 1968; Nye, 1981). In soils with pH-dependent surface charge, an increase in pH tends to make the surface charge more negative and less P-sorbing (Barrow, 2017; Penn & Camberato, 2019). Hence, P becomes more plant available.

Finally, mycorrhizal fungi and effects of the rhizosphere microbiome. Wissuwa et al. (2020) assessed the effects of mycorrhizal colonization on P uptake by efficient and inefficient genotypes of upland rice in strongly P-sorbing soil. Differences in mycorrhizal colonization—and expression of a mycorrhiza-induced P transporter (OsPT11) confirming that the symbiosis was functional—could not explain the genotypic variation in uptake per unit root surface area. Efficient genotypes always out-performed inefficient ones, independent of soil sterilization and inoculation treatments. This indicates that plant-specific factors rather than mycorrhizal fungi or other soil microbiome effects were responsible for the greater root efficiency. Though free-living microbes may solubilize P to some extent, there is little known to build a model, and any P solubilized at a distance from a root must get to a root surface.

To quantify the importance of these various factors for P acquisition by upland rice, we developed a new rhizosphere model and a method for up-scaling to the whole plant and tested it against experimental data. This is the first published model to allow for interaction between root morphology and root-induced solubilization processes. We use it to ask (1) if solubilization by pH changes can quantitatively explain the measured P uptake by genotype DJ123; (2) how sensitive P uptake would be to variations in root and soil parameters, and thereby how root morphology contributes to P uptake; and (3) how much the individual root classes contribute to uptake, particularly the metabolically cheap S-types.

2 | MATERIALS AND METHODS

2.1 | Model overview

We simulate uptake of P and efflux of HCO_3^- across root surfaces in conjunction with their transport in the rhizosphere, radially symmetrical to the root axis (Figure 1a). The HCO_3^- efflux balances the excess intake of nutrient anions (NO_3^-, $H_2PO_4^-$, SO_4^{2-}) over cations (NH_4^+, K^+, Ca^{2+}, Mg^{2+}). Reaction of HCO_3^- with the soil increases the soil pH and the concentration of P in the soil solution, and hence P availability. In the soil solid, we consider three P concentrations, pools, differing in their rates and pH-dependencies of sorption (Figure 1b).

We distinguish three root classes characteristic of rice: crown roots, (long) L-type and (short) S-type laterals, all with hairs. We include seminal roots with the crown roots because the distinction is experimentally difficult in older plants. We treat the S-types as HCO_3^--sources and P-sinks in the rhizospheres of crown roots and L-types. The uptake in the rhizosphere of unit length of crown roots and L-types is scaled-up to the whole root system using a function fitted to measurements of root length.

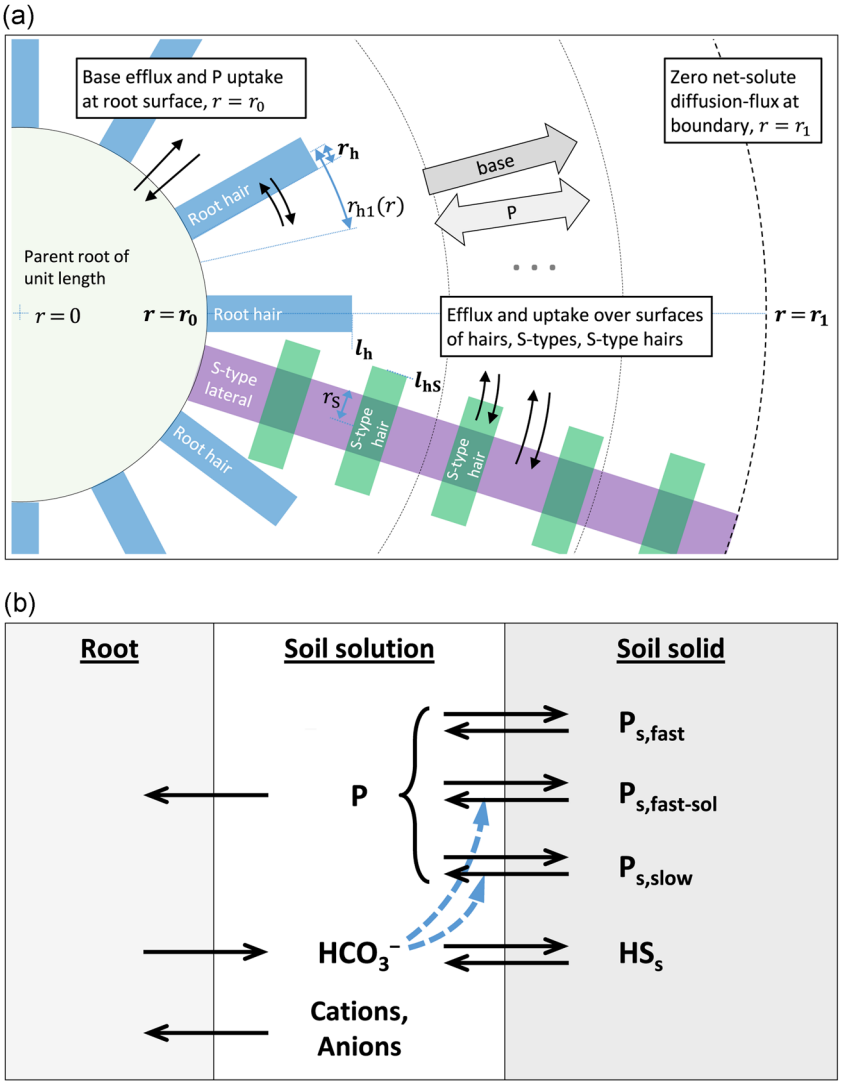


FIGURE 1 (a) The geometry of the model showing an S-type lateral and root hairs associated with a parent root (crown root or L-type lateral). (b) The interchange of P between the soil solid and solution, represented as fast and slow reactions, both sensitive to pH, and the neutralization of soil acidity by HCO_3^- released from the root, resulting in increased pH. The symbols are defined in Tables 1 and 2, and Supporting Information S1

We summarize the concepts, assumptions, and main equations in the following sections. Full details of the formulas and derivations are given in Supporting Information S1. The main symbols are defined in Table 1.

2.2 | pH gradients in the rhizosphere

Release of the base HCO_3^- from the root neutralizes soil acidity and thereby increases the soil pH, and the pH increase is dispersed through the soil by movement of acids towards the root and bases away from it. The dominant acid–base pairs are H_3O^+–H_2O and H_2CO_3–HCO_3^- in equilibrium with CO_2 in the soil air (Nye, 1981). We assume that the changes in P concentration have a negligible effect on the pH because they are far smaller than the changes in acidity. We express the pH changes in terms of acidity changes with the soil pH buffer power b_{HS}, and we express changes in pH and H_3O^+ in terms of HCO_3^- with a coefficient K, which includes the CO_2 pressure in the soil air.

At the inner boundary of the rhizosphere (i.e., the crown or L-type root surface at radius $r = r_0$), we prescribe the flux of acidity as equal to the HCO_3^- efflux. At the outer boundary ($r = r_1$), there is no flux of acidity. Thereby, we mirror neighbouring rhizospheres. The HCO_3^- efflux from S-types and hairs is treated as a source term, E_R, accounting for the volumetric surface areas of S-type and hairs. Thereby, we obtain the following equations for change in HCO_3^- concentration in the rhizosphere:

$$\frac{\partial B_\ell}{\partial t} = \frac{B_\ell \ln 10}{b_{HS}}\left[\frac{1}{r}\frac{\partial}{\partial r}\left(r\theta f\left(\frac{D_H K}{B_\ell^2} + D_B\right)\frac{\partial B_\ell}{\partial r}\right) + E_R\right], \quad (1)$$

$$\theta f\left(\frac{D_H K}{B_\ell^2} + D_B\right)\frac{\partial B_\ell}{\partial r} = -E \quad \text{at} \quad r = r_0, t > 0$$

$$\frac{\partial B_\ell}{\partial r} = 0 \quad \text{at} \quad r = r_1, t > 0$$

$$B_\ell = B_{\ell,\text{init}} \quad \text{at} \quad t = 0.$$

2.3 | P diffusion and reactions

The change in P concentration in soil around a crown root or L-type depends on diffusion, sorption, solubilization, and uptake rate of P in solution. This soil P concentration is $P = P_\ell + P_{s,fast} + P_{s,fast-sol} + P_{s,slow}$ (Table 1). We define the relationship between $P_{s,fast}$ and P_ℓ with a soil

TABLE 1 List of main symbols (variables and parameters)

Symbol	Description	Units	Value
P	Concentration of P in soil	mol cm^{-3} soil	
P_ℓ	Concentration of P in soil solution	mol cm^{-3} solution	
$P_{s,fast}$	Concentration of P in rapid equilibrium with solution	mol g^{-1} soil	
$P_{s,fast\text{-}sol}$	Concentration of P rapidly solubilizing as pH increases	mol g^{-1} soil	
$P_{s,slow}$	Concentration of P in slow equilibrium with solution	mol g^{-1} soil	
HS	Concentration of titratable acidity in soil	mol cm^{-3} soil	
B_ℓ	Concentration of HCO_3^- in soil solution	mol cm^{-3} solution	
E_R	HCO_3^- efflux from S-types and hairs	mol cm^{-3} soil s^{-1}	
l_R	P uptake rate of S-types and hairs	mol cm^{-3} soil s^{-1}	
r	Radial distance	cm	
b_P	Soil P buffer power, $b_P = \theta + \rho(\partial P_{s,fast}/\partial P_\ell)_{B_\ell}$	cm^3 solution cm^{-3} soil	5440
b_{HS}	Soil pH buffer power, $b_{HS} = -\partial HS/\partial pH$	mol cm^{-3} soil pH^{-1}	1×10^{-5}
θ	Soil volumetric moisture content	cm^3 solution cm^{-3} soil	0.3
ρ	Soil bulk density	g cm^{-3} soil	0.87
f	Diffusion impedance factor		0.24
D_P	$H_2PO_4^-$ diffusion coefficient in water	cm^2 s^{-1}	8.9×10^{-6}
D_B	HCO_3^- diffusion coefficient in water	cm^2 s^{-1}	1.23×10^{-5}
D_H	H_3O^+ diffusion coefficient in water	cm^2 s^{-1}	9.55×10^{-5}
α	Fraction of [NaOH-P_i]		0.33
β	Fraction of $P_{s,slowinit}$ after unit pH change in equilibrium		0.4
$t_{1/2}$	Half-time of slow sorption at pH = 5.8	d	28
$t^*_{1/2}$	Half-time of slow sorption at pH = 6.86	d	2
$P_{\ell,init}$	Initial P in soil solution	mol cm^{-3} solution	8×10^{-11}
$pH_{initial}$	Initial pH (1:5 H_2O)		5.8
E	Efflux of HCO_3^- across the root surface	mol cm^{-2} s^{-1}	1.83×10^{-12}
V_{max}	Maximal P uptake rate (assumed to be fast)	mol cm^{-2} s^{-1}	8×10^{-12}
K_m	Concentration at which the uptake rate is $\frac{1}{2}V_{max}$ (assumed to be low)	mol cm^{-3}	1×10^{-9}

P buffer power b_P, and the additional P solubilized as B_ℓ increases with an interaction coefficient $\lambda = (dP_\ell/dB_\ell)_P$ (Nye, 1983).

We describe the slow sorption reaction as

$$\rho\frac{\partial P_{s,slow}}{\partial t} = \kappa_a \theta P_\ell - \kappa_d \rho P_{s,slow}, \quad (2)$$

where the rate coefficients κ_a and κ_d are functions that vary with the change in B_ℓ from its initial value according to $\kappa_a = k_1 - k_1^*(B_\ell - B_{\ell,init})$ and $\kappa_d = k_2 + k_2^*(B_\ell - B_{\ell,init})$, that is, an increase in B_ℓ results in increased desorption of the slowly reacting P. The initial condition is parameterized in Equation 9.

The uptake at the root surface ($r = r_0$) follows Michaelis–Menten kinetics, and there is no net diffusion of P across the outer boundary ($r = r_1$). The uptake by the associated S-types and root hairs is treated as a sink term, l_R. Thereby, we obtain the following equations for change in P concentration in the rhizosphere:

$$\frac{\partial P_\ell}{\partial t} = \frac{1}{b_P}\left[\frac{1}{r}\frac{\partial}{\partial r}\left(rD_P\theta f\frac{\partial P_\ell}{\partial r}\right) - l_R - \rho\frac{\partial P_{s,slow}}{\partial t}\right] + \lambda\frac{\partial B_\ell}{\partial t}, \quad (3)$$

$$\begin{aligned} D_P\theta f\frac{\partial P_\ell}{\partial r} &= \frac{V_{max}P_\ell}{K_m + P_\ell} \quad \text{at} \quad r = r_0,\ t > 0 \\ \frac{\partial P_\ell}{\partial r} &= 0 \quad \text{at} \quad r = r_1,\ t > 0 \\ P_\ell &= P_{\ell,init} \quad \text{at} \quad t = 0. \end{aligned}$$

2.4 | P uptake per segment and upscaling

While integrating Equation 3, we also obtain the uptake by the root surfaces per unit length at $r = r_0$ and S-types and hairs inside the

Parameter	Symbols	S-type laterals	L-type laterals	Crown roots
Root radius (cm)	r_S, r_0	0.0025	0.01	0.03
Outer radius based on RLD (cm)	r_{S1}, r_1	Equation S26	0.339	0.339
Number of hairs per unit root length (cm^{-1})	N_{hS}, N_h	520	700	1440
Root hair length (cm)	l_{hS}, l_h	0.0125	0.014	0.02
Root hair radius (cm)	r_h	0.0008	0.0008	0.0008
Proportion of total length	ω_i	0.5	0.33	0.17
Proportion of total surface area	-	0.21	0.31	0.48

Abbreviation: RLD, root length density.

TABLE 2 Root morphology parameters based on data of Nestler et al. (2016), Kant et al. (2018), Kim et al. (2007), and Wissuwa et al. (2020)

TABLE 3 Soil P fractions

Fraction	Content (µmol g^{-1})
Resin-P	0.04
$NaHCO_3$-P_i	0.46
$NaHCO_3$-P_o	0.71
NaOH-P_i	11.29
NaOH-P_o	5.72
HCl-P	0.74
Residual-P	21.06
Total	40.02

rhizosphere (see Supporting Information S1 and Kuppe et al., 2021). The cumulative uptake per unit root length (U) at time t is the time-integral of the uptake rate ($\dot{U}$). We take root growth into account, that is, age distribution at each t. The root-length emerging at t_i can cumulate uptake only over $t - t_i$ days. Hence, the total P-uptake over time is defined as the cumulative uptake by the dynamic root system:

$$\mathcal{P}(t) = \int_0^t \dot{L}(s) \int_0^{t-s} \dot{U}(\tau) d\tau ds, \quad (4)$$

where L is the root length and $\dot{L}(t) = dL/dt$ the growth rate (Cushman, 1979). Because the length per root class is proportional to L, the total root system uptake is given by the weighted sum of the root classes, L-type, and crown root, with their U as the sum of the uptake by the root, its S-types and hairs ($U = U_{hairs} + U_{surf} + U_{S,surf} + U_{S,hairs}$), see Supporting Information S1.

To the measured root length, we fitted the function

$$L(t) = \frac{a \exp(t)}{(c + \exp(t))^b}, \quad (5)$$

with parameters a, b, and c using least-square means (Figure 2a). This function is able to fit the experimentally observed growth jump after day 7.

We assume that the crown and lateral roots experience the same initial soil concentrations $B_{\ell,init}$, $P_{\ell,init}$, $P_{s,fast,init}$, $P_{s,fast\text{-}sol,init}$, and $P_{s,slow,init}$. We assume that the distribution of root length across the root types is constant over time.

2.5 | Parameterization

2.5.1 | Plant growth and P uptake

Wissuwa et al. (2020) measured time courses of root length and P concentrations in shoot and root of rice genotype DJ123 grown on a strongly P-sorbing volcanic ash soil (Andosol) in Tsukuba, Japan. Plants were grown in a field under aerobic upland conditions or in large 72-L boxes filled with soil from the same field. Roots were collected from the field to 30-cm depth (typically sufficient for 90% of the roots—Mori et al., 2016) at 16, 28, and 48 days after emergence (DAE), and from the entire box at 7, 14, 21, and 28 DAE. Roots were scanned and analysed using the WinRHIZO software, with diameter settings of 0–0.009, 0.009–0.025, and 0.025–0.1 cm for S-type, L-type, and crown roots, respectively. By 28 DAE, the roots in boxes were too large to be scanned and total root length was estimated based on root dry weight and conversion factors determined from previous scans. Shoot samples were taken at the same times as roots, their P concentrations determined the quantity of P taken up.

The length of S-types on a segment of unit length is given by $L_{SR} = \omega_S/(\omega_C + \omega_L)$. We assumed the same L_{SR} for crown roots and L-types. Over the root length density (RLD), we computed the mid-point between neighbouring roots as outer radius assigned to a crown root or lateral

$$r_1 = \sqrt{\frac{1 + L_{SR}}{\pi \cdot RLD}}. \quad (6)$$

Equations for the mid-points concerning root hairs and S-types (r_{h1}, r_{hS1}, r_{S1}) are in the Supporting Information S1. We calculated the RLD by dividing the total length of roots per plant in the field experiment (2.5×10^4 cm) by a nominal rooting volume based on the

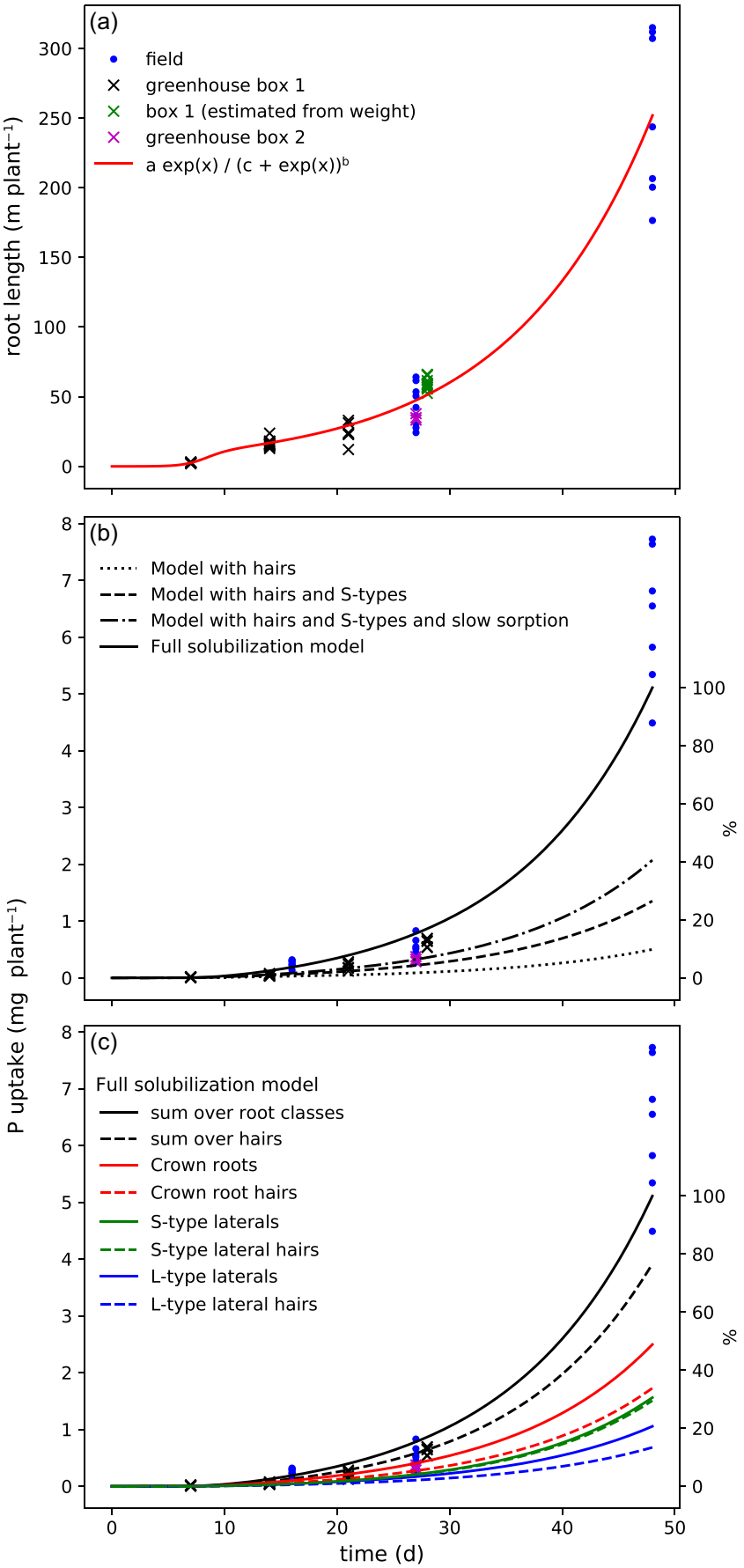


FIGURE 2 (a) Measured time course of root system length (points) and the fitted function $L(t) = a\exp(t)/(c + \exp(t))^b$ with parameters $a = 555$, $b = 0.92$, $c = 3627$ ($R^2 = 0.928$). (b) Simulated P uptake with (solid line) or without (dashed lines) solubilization, and with and without S-type laterals (21% less surface area) and slow P desorption. (c) Simulated contributions of individual root classes including their root hairs (solid lines) and their hairs only (dashed lines) to P uptake

plant spacing (10 cm × 15 cm per plant) and rooting depth (30 cm), giving RLD = 5.55 cm cm^{-3}.

Nestler et al. (2016) and Kant et al. (2018) measured the root hair length and densities in genotype DJ123. Plants were grown in the field as above and sampled from a trench of 1-m depth perpendicular to the plant rows at day 50 after seeding. Intact roots were removed by washing and stored at 4°C in 50% ethanol before root hair evaluation. Using the longest crown root of a plant, 1-cm long sections at 1, 10, 15, 20, and 25 cm from the root tip were imaged to determine root hair length and density on the crown root and its laterals. The root hair diameter was estimated from scanning electron microscope images of Kim et al. (2007).

2.5.2 | Uptake kinetics and efflux

We set the values of the Michaelis–Menten coefficients for P uptake such that they were not limiting, that is, the concentration in solution at the root surface was reduced to near zero and uptake was not sensitive to increases in V_{max} or decreases in K_m. The values of the Michaelis–Menten constants are assumed to be the same for the three root classes and root hairs (Table 1). Given that the P concentrations in the soil solution are very low, the uptake depends on the initial slope of the Michaelis–Menten function: $V(P_\ell) = V_{max}P_\ell/(K_m + P_\ell)$. For $K_m >> P_\ell$ or $P_\ell \to 0$, the ratio of V_{max} and K_m gives, approximately, the relevant slope.

We estimated the HCO_3^- efflux per unit root surface area based on the measured plant growth and estimated nutrient intakes. Shoot and root dry weight increased by 4.5 g plant^{-1} between 28 and 48 DAE (Wissuwa et al., 2020). We used the following typical nutrient contents for rice during vegetative growth (Dobermann & Fairhurst, 2000): N, K, Ca, Mg, S, P = 30, 20, 3, 2, 2, 1 mg g^{-1}, respectively. Assuming all the N was taken up as NO_3^-, which is reasonable because nitrification is rapid in this soil under the conditions of the experiment (Nardi et al., 2013), the uptake of cations was 4 mmol$_c$ plant^{-1}, and that of anions was 10.7 mmol$_c$ plant^{-1}, giving an anion excess of 6.7 mmol$_c$ plant^{-1}. Dividing this by the time-integral of root surface area (cm^2 s) gives HCO_3^- efflux = 1.83 × 10^{-12} mol cm^{-2} s^{-1}. The upscaled HCO_3^- efflux fitted the data well (R^2 = 0.93, Figure S1).

2.5.3 | Soil parameters

The basic soil properties were: clay = 17%, silt = 43%, organic C = 4.7% and initial pH (1:5 H_2O) = 5.8. We measured P fractions in the soil solid using the Hedley et al. (1982) sequential fractionation scheme as follows. (1) Resin-P by shaking 1.0 g of soil for 16 h with a strip of HCO_3^--form anion exchange resin membrane (adsorption capacity 26 µmol per strip) in H_2O, recovering P from the resin by extraction in 0.5 M HCl; (2) $NaHCO_3$-P by shaking the residue with 30 cm^3 of 0.5 M $NaHCO_3$, followed by digestion in H_2SO_4 and H_2O_2; (3) NaOH-P by shaking the residue with 30 cm^3 of 0.1 M NaOH, followed by digestion of the extract in H_2SO_4 and H_2O_2; and (4) HCl-P by shaking the residue with 30 cm^3 of 1 M HCl; and (5) Residual-P by digesting the residue in H_2SO_4 and H_2O_2. Total P in the $NaHCO_3$ and NaOH extracts was obtained from P in the digested extract; organic P (P_o) was inferred from the total P less the inorganic P (P_i) measured in the undigested extracts. P concentrations in the extracts were measured by the molybdenum blue method (Murphy & Riley, 1962). The values are in Table 3.

We calculated the initial concentrations of the soil P pools from the measured P fractions as follows. We assume [Resin-P] and [$NaHCO_3$-P_i] are in rapid equilibrium with the soil solution, and an additional proportion α of [NaOH-P_i] is rapidly released if the pH is raised by one unit. Hence, the initial $P_{s,fast}$ and $P_{s,fast\text{-}sol}$ are

$$P_{s,fast,init} = [\text{Resin-P}] + [\text{NaHCO}_3\text{-P}_i], \quad (7)$$

$$P_{s,fast\text{-}sol,init} = \alpha[\text{NaOH-P}_i]. \quad (8)$$

The initial $P_{s,slow}$ is the component of [NaOH-P_i] that slowly equilibrates:

$$P_{s,slow,init} = (1-\alpha)[\text{NaOH-P}_i]. \quad (9)$$

We define

$$P^*_{s,slow} = \beta P_{s,slow,init}, \quad (10)$$

where $P^*_{s,slow}$ is the concentration in steady-state at pH = $pH_{initial}$+1. From α, β, $t_{1/2}$, and $t^*_{1/2}$, we calculate the sorption rate coefficients in Equation 2 (Supporting Information S1), from the initial P_ℓ and $P_{s,fast}$, the soil P buffer power. From α, we calculate the interaction coefficient of B_ℓ with P_ℓ, here $\lambda = \alpha\rho[\text{NaOH-P}_i]/(b_P\Delta B^*_\ell)$, that is, solubilization concerning ΔB^*_ℓ (the change in B_ℓ above the initial value).

We measured the initial P concentration in the soil solution as follows. Portions (120 g) of air-dry soil were moistened to 50% of field capacity with deionized water and incubated in sealed containers at approximately 20°C for 21 days. The moist soil was then centrifuged and the supernatant filtered through 0.45 µm filters (Whatman). Filtered supernatant (approximately 30 cm^3) was shaken with a DGT device (DGT Research Ltd.) for 24 h, and the P adsorbed on the DGT ferrihydrite gel was desorbed into 1 cm^3 of 1 M HCl for 24 h, and measured colorimetrically.

We measured the soil pH buffer power by shaking 2 g portions of the soil in 10 cm^3 of 10 mM $CaCl_2$ overnight with sufficient NaOH to raise the initial pH by approximately 1 unit. This gave b_{HS} = 1 × 10^{-5} mol cm^{-3} pH^{-1}. We took a typical value for CO_2 pressure in the soil air of 0.004 atm (Poorter et al., 2021).

We measured the diffusion impedance factor, f, at the bulk density and moisture content of the experiments by following the

diffusion of a trace amount of non-adsorbed Br^- applied on one end of a block of the soil (Darmovzalova et al., 2020).

2.6 | Simulations and sensitivity analysis

We simulated P uptake from the rhizospheres of unit length roots and whole plant uptake over a growth period of 48 days, using the default parameters in Table 1. We analysed the sensitivity of the model prediction to two-fold smaller and larger values of plant and soil parameters.

We kept the total HCO_3^- release constant as we varied the root morphological traits (Figure S1: upscaled segment efflux). Hence, the efflux per unit root surface area, E, varied with parameters that changed the root surface area. The range in parameter values was such that the pH did not change more than one unit locally. We also tested the effect of varying the total HCO_3^- release per plant.

The distance between neighbouring roots decreases as the RLD increases. Note the inverse quadratic relationship of RLD and r_1. In the model, this also decreases the distances among S-type laterals.

We varied the length of crown roots and L-types while keeping the length of S-types per unit length of parent root, and the number of root hairs per unit root surface area, constant. Hence, a change in the length of crown roots and L-types implied a change in the total S-type length but not S-type branching density.

We tested the effect of varying the length of S-types per unit length of parent root with constraining (1) the root system length, (2) the root surface area, (3) the root volume, or (4) unconstrained. Note, the relationship between L_{SR} and r_1; therefore, we kept the RLD for (1–3) constant but not for (4). For simplicity, we fixed the length-ratio between L-type and crown roots, ω_L/ω_C. In the rhizosphere reaction term of the model, the surface area of S-types and their hairs vary as L_{SR} varies.

The total initial P concentration in soil was the same for all simulations but we varied the proportion of $P_{s,slow,init}$ and $P_{s,fast\text{-}sol,init}$, the sorption rates, and pH dependencies of sorption.

3 | RESULTS

3.1 | System P uptake

Using the default parameter set, we found that only 10% of the observed uptake could be explained without allowing for solubilization, slow sorption, and S-types (Figure 2b). Including the S-type laterals and their root hairs as additional root-morphological features increased uptake significantly (2.6-times more than without S-type laterals), but not sufficiently, the uptake was 26.4% of that of the full model with solubilization, which fits the data. Allowing all of the NaOH-P_i to contribute to slow sorption without solubilization (i.e., α = 0 in Equations 8 and 9) increased P uptake, but only to 41% of that with solubilization.

To simulate the measured uptake without solubilization and slow sorption required either a 3.6-fold increase in $P_{l,init}$ or a 224-fold increase in $P_{s,fast,init}$ (Figure S2). However, such a fast pool would lead to a soil-solution equilibrium constant, an order too high even when compared to whole inorganic P in solid phase: $1.4 \times 10^6 \gg ([\text{Resin-P}] + [\text{NaHCO}_3\text{-P}_i] + [\text{NaOH-P}_i])/P_{l,init}$. Neither of these is plausible within the uncertainty of the parameter estimates.

3.2 | Importance of different root classes

Including hairs on respective root classes, crown roots took up 48.8% of the (reference) total P-uptake compared to 30.6% for S-type laterals and 20.6% for L-type laterals (Figure 2c). The root hairs on S-types, L-types, and crown roots in sum were responsible for almost 77% of the total uptake (black dashed line), where those on crown root and S-types mattered most with a combined uptake of approximately 64% of the total. The results seem surprising, as it is generally thought that most P is taken up by lateral roots. This is still the case, but the lateral roots are here split over two classes: S- and L-types. To understand these results for the root system, we have to take a look at the cumulative uptake per unit length of crown and L-type lateral roots (Figure 3a vs. 3b).

Cumulative uptake of P per unit root length by a crown root was 3.1-times that of an L-type lateral. This can be understood by considering that a crown root has three times the surface area per unit length with about double the number of root hairs. For crown roots, most of the uptake was achieved by the hairs of the crown root itself, whereas in the rhizosphere of L-type laterals, most of the uptake was by the root hairs on their S-type laterals. Very little was taken up over the S-type root surface. Hence, the root hair contribution to uptake increased when the main root radius decreased.

In models without solubilization, the P concentration is slowly depleted and the cumulative uptake levels off or becomes approximately linear since it only depends on the uptake from a buffered P solution. In our simulations, however, more P dissolved and the P uptake by S-type hairs increased exponentially over time (compare the convex shape of dashed blue line vs. the concave shape of the dashed cyan line in Figure 3a). Consequently, the cumulative uptake did not level off. The uptake rate even accelerated somewhat at later time points for S-type hairs while it slowed down slightly for crown root hairs. S-types by themselves did not achieve the necessary pH change (data not shown; separate uptake by S-types, Figure S3), just like L-type laterals achieved a smaller pH change in their rhizosphere compared to crown roots. P uptake by S-type laterals depended on the efflux zone of the crown and L-type lateral roots.

3.3 | Rhizosphere P concentration profiles

Of importance to P-uptake is the concentration in the soil solution, P_l, which is very small, but its dynamics follow $P_{s,fast}$ (Figure 3c,d). The

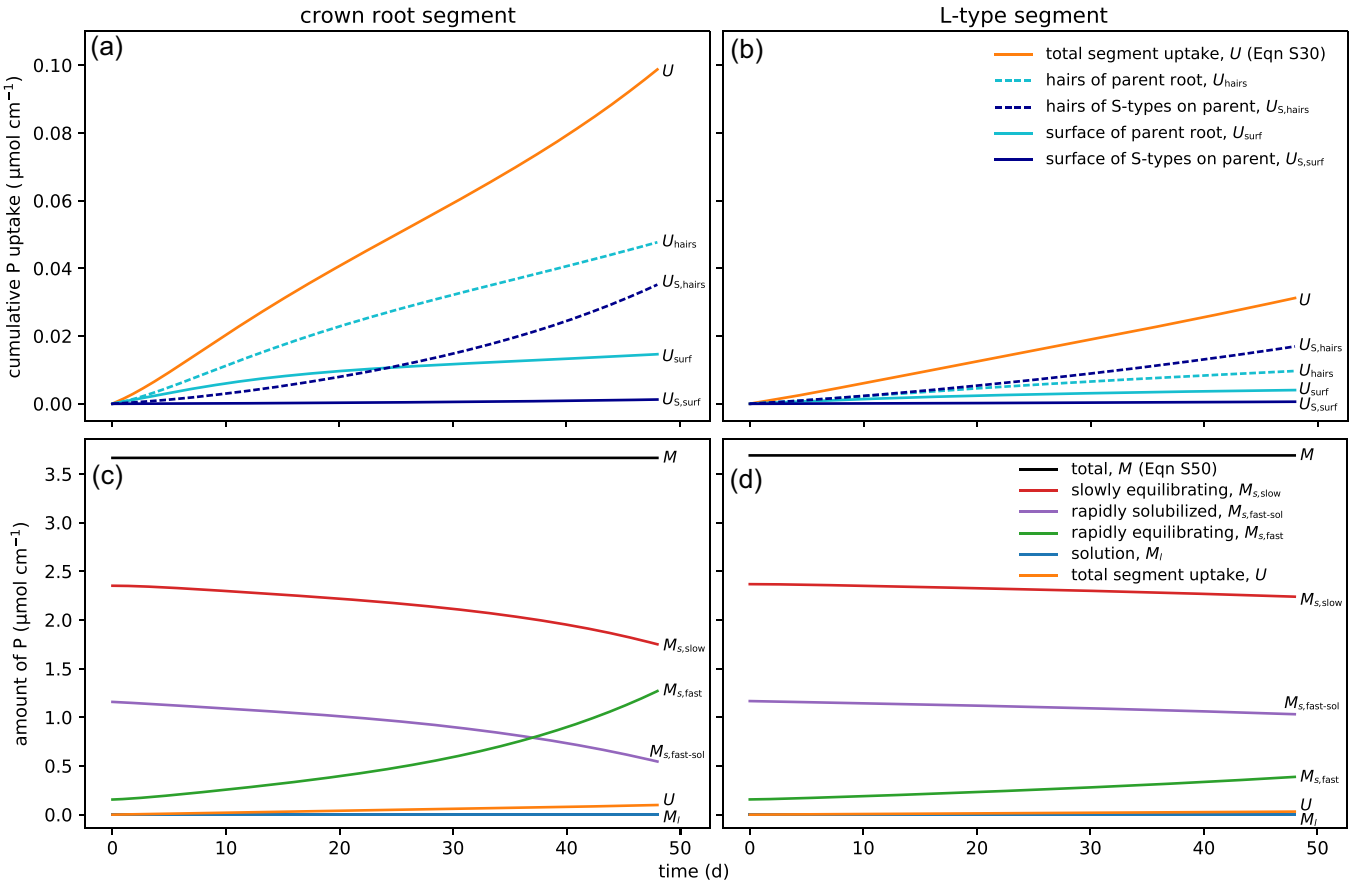


FIGURE 3 Cumulative P uptake by the surface, hairs, and S-types of crown roots (a) and L-type laterals (b) of unit length; and the amount of P in the rhizosphere volume of crown roots (c) and L-type laterals (d). Calculations are in Supporting Information S1

spatial-temporal variation in P_l (Figure 4a,b) shows that P_l was quickly depleted close to the parent root surface. This depletion zone, however, was rather narrow (<0.5 mm). For Figure 4, note that the root center is located at $r = 0$ and the root surface at $r = r_0$ (for crown roots $r_0 = 0.03$ and for L-type laterals $r_0 = 0.01$ cm, Table 2). P_l was greatly increased one mm away from the root surface. The increase of up to ten times the initial P_l concentration seems dramatic, but the resulting 0.8 µM P is still a very low concentration, normally considered highly growth limiting (Tinker & Nye, 2000). The root hairs increase plant P uptake most when placed where the P_l -increase is the greatest. The measured length of the hairs on the crown and lateral roots were not large enough to reach that zone (Table 2), but the hairs on the S-type laterals were placed across the rhizosphere.

The root and the sorbing soil pools competed for P in solution, as shown in the P balances in Figure 3c,d. Note that the uptake plotted in Figure 3a,b formed only a very small fraction of the total P concentration in the crown- and L-type lateral rhizospheres. The pools of $P_{s,slow}$ (red line) and $P_{s,fast\text{-}sol}$ (purple line) were depleted at a much greater rate than the rate at which P was taken up because the pool of $P_{s,fast}$ (green line) adsorbed a large fraction of the released P. The movement between P fractions was largely driven by the pH change.

Crown roots achieved a greater pH change in the rhizosphere: at the root surface up to +1.05 pH units and at the outer boundary up to +0.76 units (Figure 3c,d). The greater pH change in the rhizosphere of crown roots was associated with their larger surface area (i.e., diameter and number of root hairs).

3.4 | Sensitivity analysis

We analysed the sensitivity of the P uptake to a relative change in the default parameter values (Figures 5 and 6, note the log-log scale). Sensitive parameters are indicated by steep slopes and need to be determined accurately. They also present opportunities for increasing P uptake if the parameter values can be changed through breeding or agricultural management.

3.4.1 | Plant parameters

The radius r_1 is the radial distance to the mid-point between neighbouring roots in the radial model. Reducing r_1 (which corresponds with an increase in RLD) increased the local pH change and the solubilization, especially in the case of crown roots. Hence, crown roots closer together take up more P. We excluded simulations with a change in pH of more than one unit as this

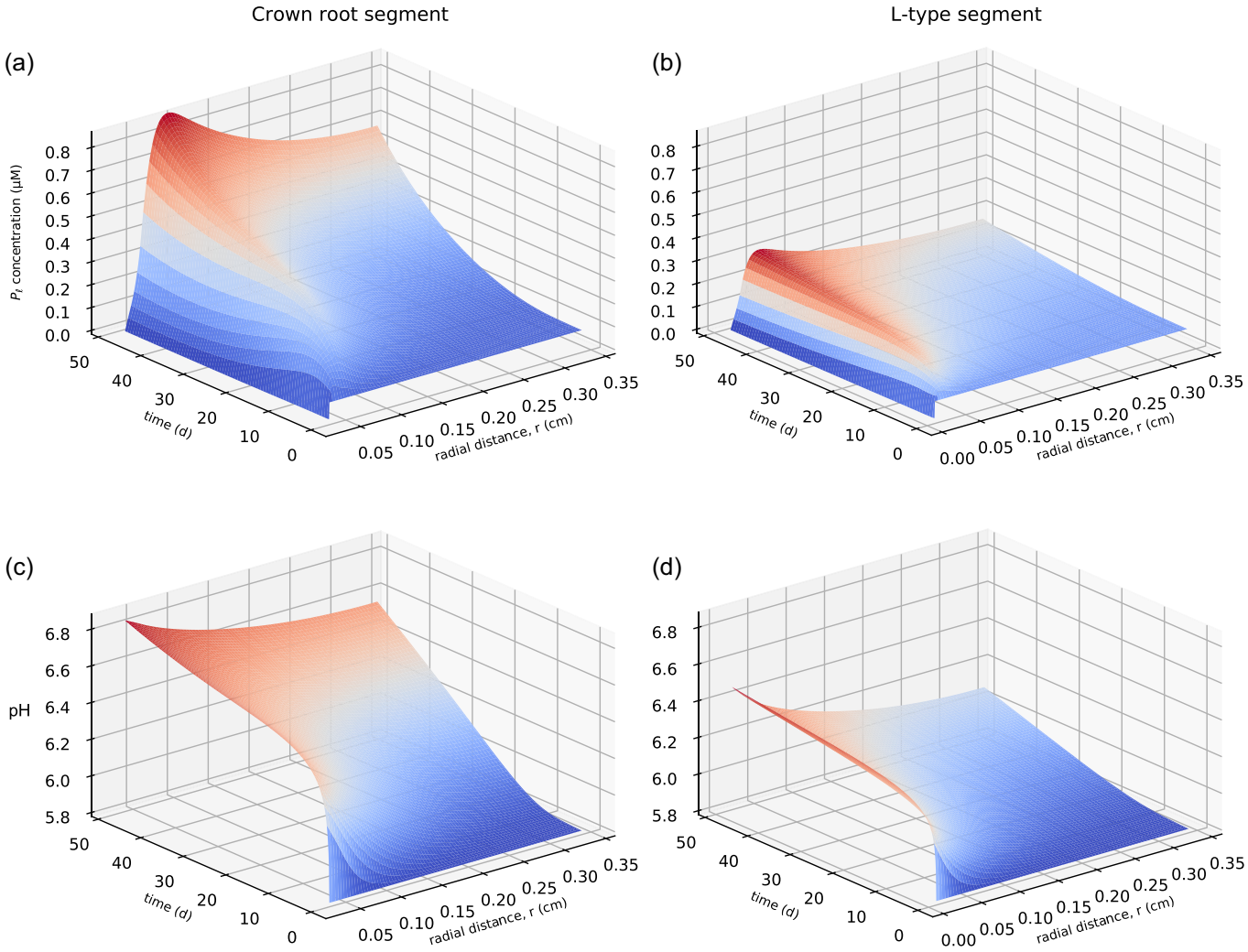


FIGURE 4 Concentration profiles over time and radial distance of (a), (b) P in the soil solution and (c), (d) pH for crown roots and L-type laterals, respectively. Model parameters are given in Tables 1 and 2. Note that the center of the segment is located at $r = 0$ and the root surface at $r = r_0$. Colours follow the contour lines

would be outside the validity of the parameter ranges. Therefore, r_1 could be reduced by 40% to approximately $r_1 = 0.2$ cm for the rhizosphere of L-type segments, obtaining 10 times the initial P_l locally (or here maximally by 45% to $r_1 = 0.186$ cm with 17.5 times $P_{l,\text{init}}$). Thus, intra-root facilitation increases with increasing RLD (Figure 5).

Among the root parameters, morphological traits influence P uptake most (root hair length l_h, root hair number N_h, root hair radius r_h, and S-type length L_{SR}, Figure 5a,b). Uptake by the root system was highly sensitive to root hair morphology (l_h, N_h, and r_h), with root hair length and number equally important (Figure 6). Uptake by L-type laterals was more sensitive than uptake by crown roots concerning change in root hair number, root hair radius, and S-type length (Figure 5a,b). The results suggest that there is more potential to increase the benefit of L-types. However, these sensitivity differences diminish at the whole root system level, because the contribution of uptake by L-type laterals to total uptake was less than that by thicker crown roots.

Besides root morphology, the root-induced HCO_3^- efflux was very important in the model. The sensitivity to the efflux was in the range of the root morphological parameters for L-types (pink line in Figure 5a,b). Additional S-types in the rhizosphere were beneficial (brown line).

3.4.2 | Soil parameters

We recap that α denotes the fraction of NaOH-P_i, which dissolves when the pH increases, and β the ratio of the slow pools in steady-state at initial pH and unit pH increase. The parameters α and β are estimated, not measured. However, the simulated uptake was not sensitive to them (Figure 5c,d). Insensitivity to α means that the pools of $P_{s,\text{fast-sol}}$ and $P_{s,\text{slow}}$ can replace each other. For example, the extreme case $\alpha = 1$ (no slow sorption) could compensate for the lack of a slow pH-dependent sorption (Figure S2).

For the variation in slow sorption, we varied the reaction half-times with and without unit pH change ($t_{1/2}$ and $t^*_{1/2}$, Equations S46 and S47).

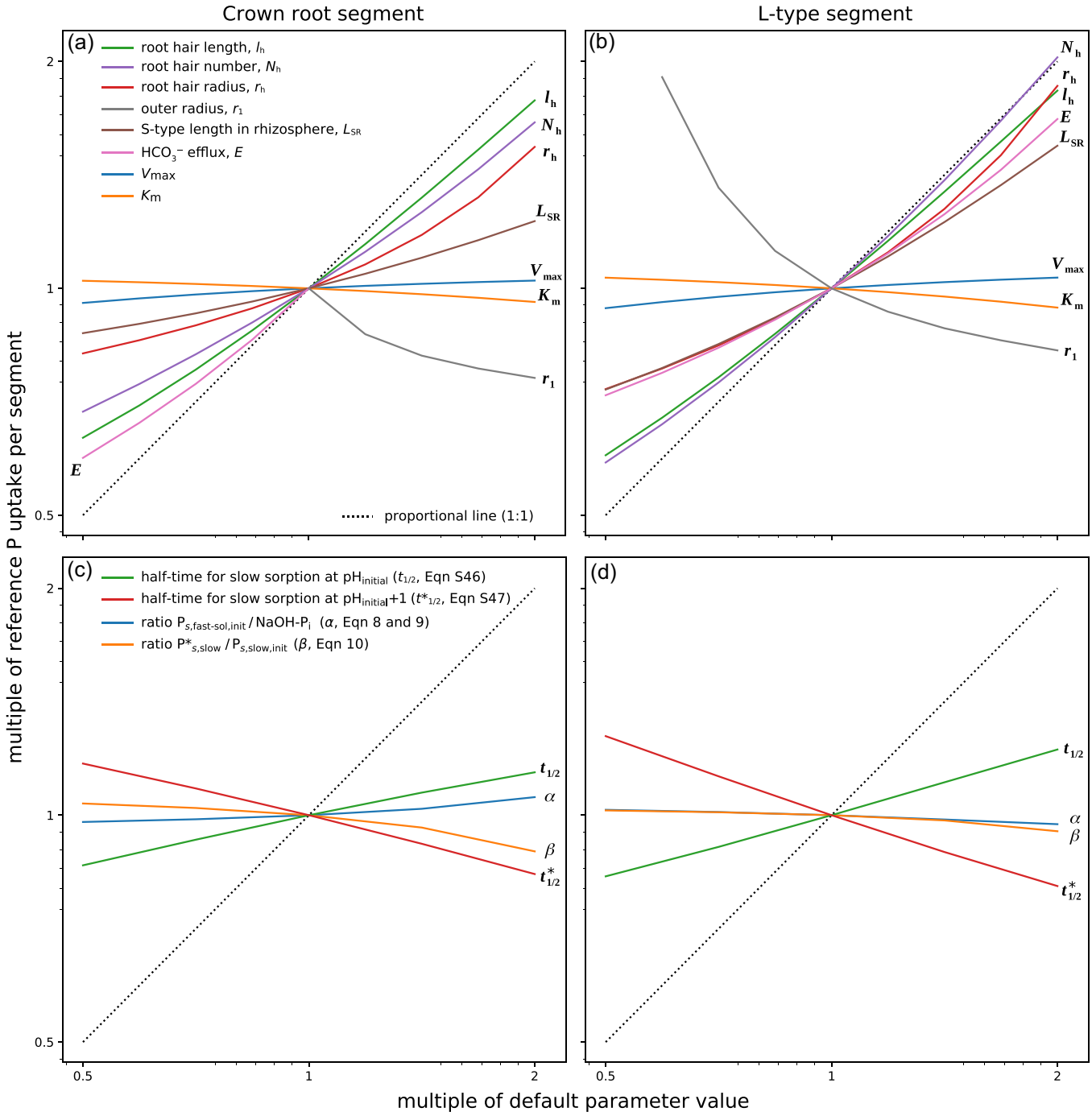


FIGURE 5 Sensitivity of P uptake per unit root length to model parameters as multiples of the standard values: (a), (b) root parameters; (c), (d) soil parameters for crown roots and L-type laterals, respectively. Note, the total release of HCO_3^- per plant is fixed for surface area variations. The initial concentration of P in soil is the same in all simulations. The outer radius r_1 and efflux are varied in a range without changing the pH locally by more than one unit (pink and grey line). Note axes are logarithmic

The uptake increased when the starting half-time ($t_{1/2}$) of the slow pool increased or when the end half-time ($t^*_{1/2}$) decreased. A smaller $t^*_{1/2}$ led to greater depletion of the slow pool. The accelerated release in response to increased pH (i.e., the discrepancy between $t_{1/2}$ and $t^*_{1/2}$) influenced uptake strongly. Hence, $t_{1/2}$ and $t^*_{1/2}$ should be determined carefully to obtain accurate predictions. For example, an accelerated slow pH-dependent desorption could compensate for the lack of rapid solubilization (Figure S2). Decreasing $t^*_{1/2}$ to 1 day resulted in approximately 130% of the reference uptake (while α = 0), and decreasing $t_{1/2}$ to 14 days with $t^*_{1/2}$= 2 days resulted in approximately 90% of the reference uptake (α = 0).

We found that the fast and slow sorbing P pools (i.e., $P_{s,fast}$ and $P_{s,slow}$) compete for the P in solution, and the extent of this competition depends on the relative rates of the fast

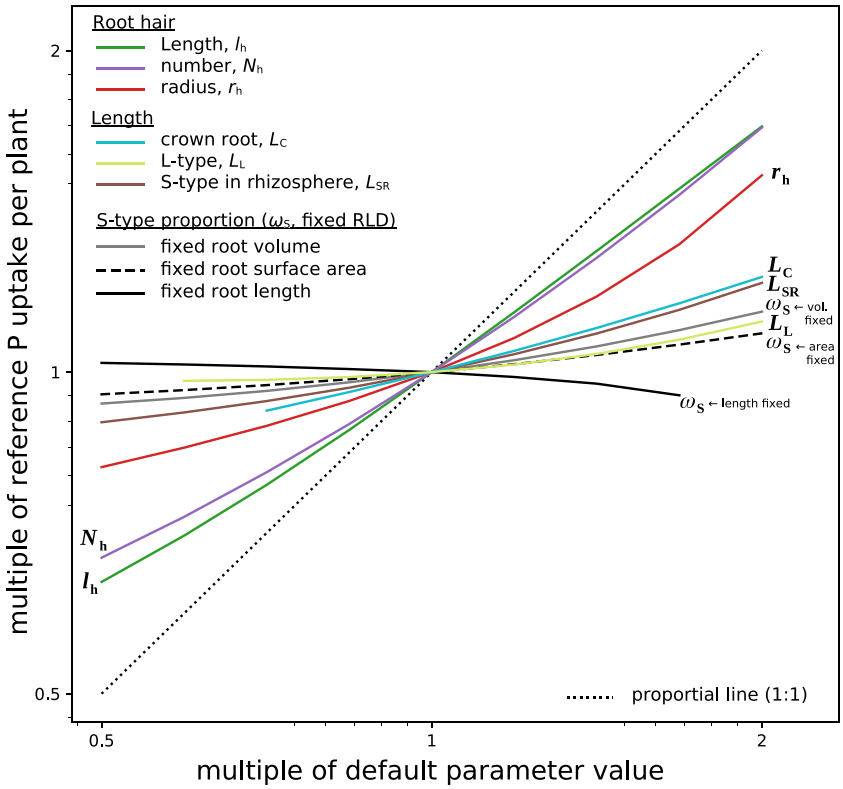


FIGURE 6 Sensitivity of total P-uptake by the root system to model parameters as multiples of the standard values. Note axes are logarithmic

and slow adsorption-desorption reactions. Therefore, we specified a relatively large pH-dependent desorption rate to overcome the competition of slow and fast P pools by depleting the slow P pool.

3.4.3 | Sensitivity of root system uptake

The total P-uptake by the root system was less sensitive to the lengths of S-types, L-types, and crown roots (L_{SR}, L_L, and L_C) than to the root hair morphology (Figure 6). While the root length increased, the released HCO_3^- per segment decreased, and thereby the uptake. Hence, the resulting sensitivity was less than the 1:1-line. The sensitivity of uptake to L_C was greater than that to L_L and about the same as to L_{SR} in the rhizospheres of both parent roots. Note that the change in L_C, and L_L implied change in total S-type length.

Changing the relative proportions of S-type to L-type to crown root (volume, surface area, or length) did not affect uptake strongly (Figure 6). Increasing the proportion of the length of S-type laterals (ω_S) relative to the other two root classes affected uptake the least and slightly negative (solid black line, condition: $\omega_S + \omega_L + \omega_C = 1$). Because an increase in S-type length at the cost of L-types (ω_L) and crown roots (ω_C) reduces the total surface area and volume of the whole root system. The direct effect of smaller surface area on P uptake is moderated by the effect on HCO_3^- efflux, which is increased since the total HCO_3^- release per plant is fixed. Usually, trade-offs for investment into root classes are presented on a metabolic equivalence basis, either in terms of carbon or P. We do not know these costs in our system, but we may compare root system compositions with varying S-type lengths at a fixed total root surface area (dashed black line in Figure 6) or volume (grey line). Note that keeping surface area or volume fixed, an increase in ω_S increases the total root length ($\omega_S + \omega_L + \omega_C \neq 1$). Furthermore, we kept the RLD fixed by varying r_1. An increase in S-type proportion but fixed total root surface area or volume resulted in only slightly more P uptake. Hence, the investment between S-types and thicker root classes seems balanced in DJ123.

4 | DISCUSSION

4.1 | The importance of solubilization and its interaction with root morphology

Conventional models of P uptake in which roots are treated as sinks for P, but not otherwise influencing the solubility of P in the soil, work reasonably well for soils with large P concentrations in the soil solution. But for strongly P-sorbing soils, such as highly weathered soils of the humid tropics and volcanic ash soils, such models tend to greatly underestimate uptake. Hence, the model without solubilization could only account for 41% of the observed uptake (Figure 2b). The full model allows for solubilization of P and interactions between solubilization and root morphology. The full model successfully predicts the total P-uptake by the P-efficient upland rice genotype DJ123 growing in a strongly sorbing soil using input parameter values measured independently.

As P is removed from the soil by root uptake, a zone of depletion develops around the root (Figure 4). The depletion zone is narrow because P diffusion in the soil is very slow due to the strong sorption. However, simultaneously the root releases HCO_3^- ions into the soil to balance higher anion than cation intake, and the reaction of HCO_3^- with the soil tends to increase the P concentration in solution. In our simulations, HCO_3^- diffused faster than P and, consequently, a zone developed in which the P concentration in solution rose above that in the soil bulk. Thus, peaks in P concentration in solution formed at approximately 0.1 cm from the crown root and 0.06 cm from the L-type (Figure 4a,b). Phosphate, therefore, diffuses from the solubilization zone, albeit very slowly (Figure S4). This is where the interaction with fine S-type lateral roots branching off the parent root becomes important because the laterals and their hairs may intercept solubilized P that would otherwise not be available to the plant. The increase in P uptake due to solubilization is thereby reinforced.

4.2 | Root-induced pH changes

Efflux of HCO_3^- from the roots depends on the excess influx of anions over cations, which depends on the rate of increase in total plant biomass, the nutrient composition of the plant, the root-shoot ratio, and root surface area. That means, for a fixed root surface area, the total HCO_3^- release increases as the rate of plant growth increases (Figure 5a,b, pink lines). Hence, a genotype with better internal P use efficiency (greater growth rate per unit root surface) can have better P uptake efficiency due to an increased HCO_3^- efflux and P solubilization.

We estimated HCO_3^- efflux from the total biomass with a typical nutrient composition of rice and used a constant efflux per unit root surface area. Therefore, crown roots induced greater pH change than L-type laterals (Figure 4). For a given efflux, root-induced pH changes will be greater with more compact root systems. Hence, at greater RLD, the distance between neighbouring roots is smaller, and therefore the HCO_3^- accumulates in a smaller volume of soil, resulting in greater solubilization and uptake. However, this effect will be offset if the uptake of other nutrients, and hence the HCO_3^- efflux, is impaired at the greater rooting density.

Soil factors also influence the pH change away from the roots but were not studied in detail. The initial soil pH, the CO_2 pressure in the soil air, and the soil pH buffer power (Equation 1) will therefore also influence P solubilization and uptake to some extent.

4.3 | Root P uptake kinetics

We assigned values for the root P uptake parameters such that they did not limit uptake, and there was no minimum concentration below which uptake ceased. In reality, there must be some minimum concentration for P uptake transporters to operate. Rice plants can reduce solution P concentrations to 16 nM (Mori et al., 2016), however, reliable minimum concentrations are rarely documented (Griffiths & York, 2020). If the P transporter activity limited uptake to some minimum concentration, additional solubilization would be required to account for the observed rates of P uptake. There is a need to measure genotypic variation in root uptake parameters in the sub-micro-molar range as it may explain (among other traits) why some genotypes have lower uptake per unit root length than more P-efficient genotypes.

4.4 | Contributions of different root classes to uptake

S-type laterals increase net P uptake dramatically because they are positioned inside the solubilization zones but outside the P depletion zones of L-types and crown roots. Although the S-types have a small diameter, their effective surface area for P uptake is greatly increased by their hairs. They are therefore efficient in intercepting P solubilized by their parent root. Over time, as the zone of pH-change and P solubilization around the parent root spreads further into the soil, the importance of S-types 'reaching out' increases. Treating S-type laterals independent of parent roots reduced their contribution to total P-uptake from 30% to 11% (Figure S3). Likewise, using a model that did not explicitly allow for solubilization, Gonzalez et al. (2021) found that S-types contributed little to total P-uptake by the root system. Nonetheless, they showed that the low P cost of forming S-type laterals can be recovered by their P uptake within a day, much faster than other root types. With a model allowing for solubilization, this period would be even shorter. This facilitation of P uptake among the root classes suggests that there needs to be a balanced investment into the different root classes to optimize uptake.

Crown roots contribute less to the total root length than other root types but much to the total root surface area because of their larger diameter (Table 2). That large surface area furthermore allows more root hairs to grow per unit root length. This explains why crown root hairs contribute most to total P-uptake. In addition to crown root uptake, their role as a parental root in enhancing P-uptake by S-type laterals is larger than for parental L-type laterals due to the greater pH change and P solubilization they cause. We conclude that crown roots have an important role in P uptake, and this may explain why genotypes with many crown roots have high performance under low P, despite crown roots being metabolically expensive (Wissuwa et al., 2020).

The total uptake by the whole root system was not sensitive to changes in the partitioning of S-type length (Figure 6, grey and brown line). This suggests that the P-efficient genotype DJ123 achieves a good balance among the root classes.

4.5 | Influence of root hair morphology on uptake

In the model, root hairs compete for P in the soil solution with the perpendicular root surface, and most of the P is taken up by hairs

(Figure 3). Overall, the simulated uptake is strongly increased in response to increased root hair length, number, and diameter (Figures 5 and 6). Zygalakis et al. (2011) found—with a model allowing for root hairs but not solubilization or S-type laterals—that hair density had a much smaller effect on the uptake than length. This was because the hairs rapidly depleted P in the soil volume between them so that increasing the hair density had little effect. In our simulations, most hairs on S-type laterals are outside of the depletion zone of the parent root but within the zone where solubilization increases the P concentration in the soil solution. Therefore, more densely spaced hairs had a similar impact to longer hairs.

Nestler and Wissuwa (2016) found that differences among upland rice genotypes were mostly due to the ability to increase hair length in response to P deficiency, and all the measured hair parameters showed consistent variation across root types. However, compared to the length of root hairs reported for other *Poaceae* species (Hill et al., 2010; Itoh & Barber, 1983; Marzec et al., 2015), rice root hairs seem short and those on the parent roots do not reach as far as the peak of solubilized P concentration. Presumably, the P returns per unit P invested are greater for hairy S-types than for longer hairs alone.

While less important than root hair length and density, we found hair radius did influence uptake (Figures 5 and 6). We are not aware of any published data on variation in root hair diameter in rice, but two-fold variation can be seen in images by Kim et al. (2007). Data from arabidopsis showed variation among genotypes exceeding variations within a given genotype (Parker et al., 2000), suggesting that variations in root hair diameter should be explored as a potential way to increase P uptake.

4.6 | Time dynamics of whole root system P uptake

The upscaled P uptake curve follows the exponential increase in measured P uptake quite nicely (Figure 2). Our simulations, however, overestimate the uptake during earlier time points and are below the measured average at the last time point. The shape of the P uptake curve for the whole root system is largely determined by the shape of the root growth curve with little influence of temporal uptake dynamics per unit root segment (Figure 3a,b). In upscaling, we account for the cumulative uptake by younger and older roots. Since the root system is a combination of older and younger roots at any time, the time dynamics of solubilization at the rhizosphere scale averages out at the whole root system scale. It proved, therefore, difficult to improve the fit of the whole root system P uptake curve by changing the model parameters. Possibly, root length was underestimated in the field experiment, where collecting whole root systems is challenging. Furthermore, additional processes may have contributed over time, such as an increase in the contribution of mycorrhizal fungi.

4.7 | Trade-offs and feedbacks at the whole plant level

At the whole plant level, there may be feedbacks that enhance growth under P-limited conditions causing small rhizosphere effects to have an increasing impact over time (Wissuwa, 2003). Greater P uptake is likely to increase growth and also the uptake of other nutrients resulting in increased HCO_3^- efflux, solubilization, and eventually P uptake. This positive feedback would benefit from greater internal P use efficiency. It would also benefit from an optimal investment into the different root classes and root hairs to capture the solubilized P. We concluded earlier that DJ123 seems balanced in this respect. However, the uptake of other nutrients, particularly nitrogen, also influences the relative investment into root classes. The best root system for capturing NO_3^- may have long crown roots exploiting the whole soil volume (Dathe et al., 2016). Such a diffuse and deep root system is likely to be less effective for P uptake. But since P uptake depends on solubilization, NO_3^- uptake is also important. Therefore, there may be trade-offs for optimizing root architecture and morphology. Further model studies are needed to explore this.

5 | CONCLUSIONS

Our mechanistic model successfully simulates P uptake by the P-efficient genotype DJ123 growing on strongly sorbing soil. The model allows the interchange of P between the soil solid and solution through fast and slow, pH-dependent reactions and for the P-solubilizing effect of root-induced pH changes. The modelled root system contains three root classes, all hairy: crown roots, L-type laterals, and S-type laterals. The simulated uptake is a result of an important interaction between solubilization and the morphology of the upland rice root system. In the absence of solubilization or S-type laterals, the model could not account for the measured uptake. P uptake is less sensitive to total root length and root class proportions. But S-types greatly enhance overall P uptake because they extend across the solubilization zone around the parent and beyond its P depletion zone. Hence, S-type laterals, longer root hairs, and greater RLD can improve uptake. However, these S-types are particularly beneficial in the solubilization zone. Solubilization over time is greater around thicker roots and when RLD is high. The greater surface area that comes with thicker roots increases the release of HCO_3^-, which relates to the plant nutrient composition and relative growth rates. Root hairs and S-types do not achieve strong solubilization themselves, but their P uptake is facilitated by the near presence of thicker roots, especially nodal roots. We thus found a pronounced facilitative interaction between very fine laterals and their thicker parent root and this needs to be considered in formulating target traits for selecting P-efficient rice cultivars.

ACKNOWLEDGEMENTS

We thank Drs. Naoki Moritsuka and Tovo Rakotoson for their help with the soil measurements. Christian W. Kuppe and Johannes A. Postma were

institutionally funded by the Helmholtz Association (POF IV: 2171, Biological and environmental resources for sustainable use). Guy J. D. Kirk was supported by BBSRC (Grant Ref. BB/R020388/1) and OCP (Cranfield-Rothamsted-UM6P Collaboration Grant). Open access fees were funded by the Deutsche Forschungsgemeinschaft (DFG, German Research Foundation) – 491111487. Open access funding enabled and organized by Projekt DEAL.

CONFLICT OF INTERESTS

The authors declare no conflict of interest.

DATA AVAILABILITY STATEMENT

Contact the corresponding author for experimental data or source code.

ORCID

Christian W. Kuppe http://orcid.org/0000-0002-1837-759X
Guy J. D. Kirk http://orcid.org/0000-0002-7739-9772
Matthias Wissuwa http://orcid.org/0000-0003-3505-9398
Johannes A. Postma http://orcid.org/0000-0002-5222-6648

REFERENCES

Alewell, C., Ringeval, B., Ballabio, C., Robinson, D.A., Panagos, P. & Borrelli, P. (2020) Global phosphorus shortage will be aggravated by soil erosion. *Nature Communications*, 11(1), 4546. Available from: https://doi.org/10.1038/s41467-020-18326-7

Barrow, N.J. (2017) The effects of pH on phosphate uptake from the soil. *Plant and Soil*, 410(1), 401–410. Available from: https://doi.org/10.1007/s11104-016-3008-9

Cushman, J.H. (1979) An analytical solution to solute transport near root surfaces for low initial concentration: I. Equations development. *Soil Science Society of America Journal*, 43, 1087–1090. Available from: https://doi.org/10.2136/sssaj1979.03615995004300060005x

Darmovzalova, J., Boghi, A., Otten, W., Eades, L.J., Roose, T., Guy, Kirk, J.D. (2020) Uranium diffusion and time-dependent adsorption–desorption in soil: a model and experimental testing of the model. *European Journal of Soil Science*, 71(2), 215–225. Available from: https://doi.org/10.1111/ejss.12814

Dathe, A., Postma, J.A., Postma-Blaauw, M.B. & Lynch, J.P. (2016) Impact of axial root growth angles on nitrogen acquisition in maize depends on environmental conditions. *Annals of Botany*, 118(3), 401–414. Available from: https://doi.org/10.1093/aob/mcw112

De Bauw, P., Hieu Mai, T., Schnepf, A., Merckx, R., Smolders, E. & Vanderborght, J. (2020) A functional–structural model of upland rice root systems reveals the importance of laterals and growing root tips for phosphate uptake from wet and dry soils. *Annals of Botany*, 126(4), 789–806. Available from: https://doi.org/10.1093/aob/mcaa120

Dijkshoorn, W., Lathwell, D.J. & De Wit, C.T. (1968) Temporal changes in carboxylate content of ryegrass with stepwise change in nutrition. *Plant and Soil*, 29(3), 369–390. Available from: https://doi.org/10.1007/BF01348971

Dobermann, A. & Fairhurst, T. (2000) *Rice: nutrient disorders & nutrient management*. International Rice Research Institute.

Gamuyao, R., Chin, J.H., Pariasca-Tanaka, J., Pesaresi, P., Catausan, S., Dalid, C. et al. (2012) The protein kinase Pstol1 from traditional rice confers tolerance of phosphorus deficiency. *Nature*, 488(7412), 535–539. Available from: https://doi.org/10.1038/nature11346

Gonzalez, D., Postma, J.A. & Wissuwa, M. (2021) Cost-benefit analysis of the upland-rice root architecture in relation to phosphate: 3D simulations the importance of S-type lateral roots for reducing the pay-off time. *Frontiers in Plant Science*, 12, 359. Available from: https://doi.org/10.3389/fpls.2021.641835

Griffiths, M. & York, L.M. (2020) Targeting root ion uptake kinetics to increase plant productivity and nutrient use efficiency. *Plant Physiology*, 182(4), 1854–1868. Available from: https://doi.org/10.1104/pp.19.01496

Hedley, M.J., Kirk, G.J.D. & Santos, M.B. (1994) Phosphorus efficiency and the forms of soil phosphorus utilized by upland rice cultivars. *Plant and Soil*, 158(1), 53–62. Available from: https://doi.org/10.1007/BF00007917

Hedley, M.J., White, R.E. & Nye, P.H. (1982) Plant-induced changes in the rhizosphere of rape (Brassica napus var. Emerald) seedlings. *New Phytologist*, 91(1), 45–56. Available from: https://doi.org/10.1111/j.1469-8137.1982.tb03291.x

Hill, J.O., Simpson, R.J., Ryan, M.H. & Chapman, D.F. (2010) Root hair morphology and mycorrhizal colonisation of pasture species in response to phosphorus and nitrogen nutrition. *Crop and Pasture Science*, 61, 122–131. Available from: https://doi.org/10.1071/CP09217

Hinsinger, P., Brauman, A., Devau, N., Gérard, F., Jourdan, C., Laclau, J.P. et al. (2011) Acquisition of phosphorus and other poorly mobile nutrients by roots. Where do plant nutrition models fail? *Plant and Soil*, 348(1), 29–61. Available from: https://doi.org/10.1007/s11104-011-0903-y

Hoffland, E. (1992) Quantitative evaluation of the role of organic acid exudation in the mobilization of rock phosphate by rape. *Plant and Soil*, 140(2), 279–289. Available from: https://doi.org/10.1007/BF00010605

Itoh, S. & Barber, S.A. (1983) Phosphorus uptake by six plant species as related to root hairs1. *Agronomy Journal*, 75(3), 457–461. Available from: https://doi.org/10.2134/agronj1983.00021962007500030010x

Kant, J., Ishizaki, T., Pariasca-Tanaka, J., Rose, T., Wissuwa, M. & Watt, M. (2018) Phosphorus efficient phenotype of rice. In: Shah, F., Khan, Z. K. & Iqbal, A. (Eds.) *Rice crop—current developments*. IntechOpen, pp. 129–148. https://doi.org/10.5772/intechopen.75642

Kim, C.M., Han Park, S., Il Je, B., Hyun Park, S.u, Park, S.J., Long Piao, H. et al. (2007) OsCSLD1, a cellulose synthase-like D1 gene, is required for root hair morphogenesis in rice. *Plant Physiology*, 143(3), 1220–1230. Available from: https://doi.org/10.1104/pp.106.091546

Kirk, G.J.D. (1999) A model of phosphate solubilization by organic anion excretion from plant roots. *European Journal of Soil Science*, 50(3), 369–378. Available from: https://doi.org/10.1111/j.1365-2389.1999.00239.x

Kirk, G.J.D., Santos, E.E. & Santos, M.B. (1999) Phosphate solubilization by organic anion excretion from rice growing in aerobic soil: rates of excretion and decomposition, effects on rhizosphere pH and effects on phosphate solubility and uptake. *New Phytologist*, 142(2), 185–200.

Kuppe, C.W., Huber, G. & Postma, J.A. (2021) Comparison of numerical methods for radial solute transport to simulate uptake by plant roots. *Rhizosphere*, 18, 100352. Available from: https://doi.org/10.1016/j.rhisph.2021.100352

Kuppe, C.W., Schnepf, A., von Lieres, E., Watt, M. & Postma, J.A. (2022) Rhizosphere models: their concepts and application to plant-soil ecosystems. *Plant and Soil*. Available from: https://doi.org/10.1007/s11104-021-05201-7

Marzec, M., Melzer, M. & Szarejko, I. (2015) Root hair development in the grasses: what we already know and what we still need to know. *Plant Physiology*, 168(2), 407–414. Available from: https://doi.org/10.1104/pp.15.00158

Mori, A., Fukuda, T., Vejchasarn, P., Nestler, J., Pariasca-Tanaka, J. & Wissuwa, M. (2016) The role of root size versus root efficiency in phosphorus acquisition in rice. *Journal of Experimental Botany*,

67(4), 1179–1189. Available from: https://doi.org/10.1093/jxb/erv557

Murphy, J. & Riley, J.P. (1962) A modified single solution method for the determination of phosphate in natural waters. *Analytica Chimica Acta*, 27, 31–36. Available from: https://doi.org/10.1016/S0003-2670(00)88444-5

Nardi, P., Akutsu, M., Pariasca-Tanaka, J. & Wissuwa, M. (2013) Effect of methyl 3-4-hydroxyphenyl propionate, a sorghum root exudate, on N dynamic, potential nitrification activity and abundance of ammonia-oxidizing bacteria and archaea. *Plant Soil*, 367, 627–637. Available from: https://doi.org/10.1007/s11104-012-1494-y

Nestler, J., Keyes, S.D. & Wissuwa, M. (2016) Root hair formation in rice (*Oryza sativa L.*) differs between root types and is altered in artificial growth conditions. *Journal of Experimental Botany*, 67(12), 3699–3708. Available from: https://doi.org/10.1093/jxb/erw115

Nestler, J. & Wissuwa, M. (2016) Superior root hair formation confers root efficiency in some, but not all, rice genotypes upon P deficiency. *Frontiers in Plant Science*, 7, 1935. Available from: https://doi.org/10.3389/fpls.2016.01935

Nye, P.H. (1981) Changes of pH across the rhizosphere induced by roots. *Plant and Soil*, 61(1), 7–26. Available from: https://doi.org/10.1007/BF02277359

Nye, P.H. (1983) The diffusion of two interacting solutes in soil. *Journal of Soil Science*, 34(4), 677–691. Available from: https://doi.org/10.1111/j.1365-2389.1983.tb01064.x

Oburger, E., Kirk, G.J.D., Wenzel, W.W., Puschenreiter, M. & Jones, D.L. (2009) Interactive effects of organic acids in the rhizosphere. *Soil Biology and Biochemistry*, 41(3), 449–457. Available from: https://doi.org/10.1016/j.soilbio.2008.10.034

Parker, J.S., Cavell, A.C., Dolan, L., Roberts, K. & Grierson, C.S. (2000) Genetic interactions during root hair morphogenesis in arabidopsis. *The Plant Cell*, 12(10), 1961–1974. Available from: https://doi.org/10.1105/tpc.12.10.1961

Penn, C.J. & Camberato, J.J. (2019) A critical review on soil chemical processes that control how soil pH affects phosphorus availability to plants. *Agriculture*, 9(6), 120. Available from: https://doi.org/10.3390/agriculture9060120

Poorter, H., Knopf, O., Wright, I.J., Temme, A.A., Hogewoning, S.W., Graf, A. et al. (2021) A meta-analysis of responses of C_3 plants to atmospheric CO_2: dose–response curves for 85 traits ranging from the molecular to the whole-plant level. *New Phytol*, 233, 1560–1596. Available from: https://doi.org/10.1111/nph.17802

Rakotoson, T., Holz, M. & Wissuwa, M. (2020) Phosphorus deficiency tolerance in *Oryza Sativa*: root and rhizosphere traits. *Rhizosphere*, 14, 100198. Available from: https://doi.org/10.1016/j.rhisph.2020.100198

Rose, T.J., Impa, S.M., Rose, M.T., Pariasca-Tanaka, J., Mori, A., Heuer, S. et al. (2013) Enhancing phosphorus and zinc acquisition efficiency in rice: a critical review of root traits and their potential utility in rice breeding. *Annals of Botany*, 112(2), 331–345. Available from: https://doi.org/10.1093/aob/mcs217

Schatz, M.C., Maron, L.G., Stein, J.C., Hernandez Wences, A., Gurtowski, J., Biggers, E. et al. (2014) Whole genome de novo assemblies of three divergent strains of rice, *Oryza sativa*, document novel gene space of aus and indica. *Genome Biology*, 15(11), 1–16. Available from: https://doi.org/10.1186/s13059-014-0506-z

Tinker, P.B. & Nye, P.H. (2000) Solute movement in the rhizosphere. *Topics in sustainable agronomy*. Oxford University Press.

Vandamme, E., Rose, T., Saito, K., Jeong, K. & Wissuwa, M. (2016) Integration of P acquisition efficiency, P utilization efficiency and low grain P concentrations into P-efficient rice genotypes for specific target environments. *Nutrient Cycling in Agroecosystems*, 104(3), 413–427. Available from: https://doi.org/10.1007/s10705-015-9716-3

Wissuwa, M. (2003) How do plants achieve tolerance to phosphorus deficiency? Small causes with big effects. *Plant Physiology*, 133(4), 1947–1958. Available from: https://doi.org/10.1104/pp.103.029306

Wissuwa, M. (2005) Combining a modelling with a genetic approach in establishing associations between genetic and physiological effects in relation to phosphorus uptake. *Plant and Soil*, 269(1), 57–68. Available from: https://doi.org/10.1007/s11104-004-2026-1

Wissuwa, M., Gonzalez, D. & Watts-Williams, S. J. (2020) The contribution of plant traits and soil microbes to phosphorus uptake from low-phosphorus soil in upland rice varieties. *Plant and Soil*, 448(1), 523–537. Available from: https://doi.org/10.1007/s11104-020-04453-z

Wissuwa, M., Kondo, K., Fukuda, T., Mori, A., Rose, M.T., Pariasca-Tanaka, J. et al. (2015) Unmasking novel loci for internal phosphorus utilization efficiency in rice germplasm through genome-wide association analysis. *PLoS One*, 10(4), e0124215. Available from: https://doi.org/10.1371/journal.pone.0124215

Yamauchi, A., Kono, Y. & Tatsumi, J. (1987) Comparison of root system structures of 13 species of cereals. *Japanese Journal of Crop Science*, 56(4), 618–631. Available from: https://doi.org/10.1626/jcs.56.618

Zygalakis, K.C., Kirk, G.J.D., Jones, D.L., Wissuwa, M. & Roose, T. (2011) A dual porosity model of nutrient uptake by root hairs. *New Phytologist*, 192(3), 676–688. Available from: https://doi.org/10.1111/j.1469-8137.2011.03840.x

SUPPORTING INFORMATION

Additional supporting information may be found in the online version of the article at the publisher's website.

How to cite this article: Kuppe, C.W., Kirk, G.J.D., Wissuwa, M. & Postma, J.A. (2022) Rice increases phosphorus uptake in strongly sorbing soils by intra-root facilitation. *Plant, Cell & Environment*, 45, 884–899. https://doi.org/10.1111/pce.14285

DSPACE

https://dspace.org/

Rice increases phosphorus uptake in strongly sorbing soils by intra-root facilitation

Kuppe, Christian W.; Kirk, Guy J. D.; Wissuwa, Matthias; Postma, Johannes A.

2022-02-09
Wiley
https://doi.org/10.1111/pce.14285
Kuppe CW, Kirk GJ, Wissuwa M, Postma JA. (2022) Rice increases phosphorus uptake in strongly sorbing soils by intra-root facilitation, Plant, Cell and Environment, Volume 45, Issue 3, February 2022, pp. 884-899

Downloaded from a DSpace repository. https://dspace.org/